Inorganic Chemistry Communications 69 (2016) 31–34

Contents lists available at ScienceDirect

Inorganic Chemistry Communications

journal homepage: www.elsevier.com/locate/inoche

Short communication

A Ni(II) ferromagnet with mixed pyridine-3,5-dicarboxylate-1,4-bis(imidazol-l-yl)butane heterobridges exhibiting long-range ordering and hysteresis loop

Min-Le Han [a,b], Xue-Qian Wu [a], Guo-Wang Xu [a], Guo-Xuan Wen [a], Dong-Sheng Li [a,*], Lu-Fang Ma [b,*]

[a] College of Materials and Chemical Engineering, Hubei Provincial Collaborative Innovation Center for New Energy Microgrid, Key Laboratory of Inorganic Nonmetallic Crystalline and Energy Conversion Materials, China Three Gorges University, Yichang 443002, PR China

[b] College of Chemistry and Chemical Engineering, Henan Key Laboratory of Function-Oriented Porous Materials, Luoyang Normal University, Luoyang 471022, PR China

ARTICLE INFO

Article history:
Received 20 March 2016
Received in revised form 17 April 2016
Accepted 21 April 2016
Available online 22 April 2016

Keywords:
Ni^{II}-CPs
Pyridine-3,5-dicarboxylic acid
1,4-bis(imidazol-l-yl)butane
Magnetic property

ABSTRACT

A rare Ni-ferromagnet $[Ni(pdc)(bib)]\cdot 2H_2O$ (H_2pdc = pyridine-3,5-dicarboxylic acid, bib = 1,4-bis (imidazol-l-yl) butane) has been prepared, which possesses a 3D supramolecular network based on (3,5)-connected helical-armed 2D layers. Interestingly, at high temperature (>12.7 K), **1** exhibits a weak ferromagnetism, whereas at low temperature, it shows unusual long-range ordering (LRO) behaviors combining spin canting and hysteresis loop.

Coordination polymers (CPs) based on parmagnetic metal ions exhibiting extended structures are of intense current interest in the field of molecular magnetism and materials chemistry due to their various structural topologies and potential applications as functional materials [1–5]. These materials have also offered great opportunities to better understand fundamental magnetic phenomena, such as long-range ordering (LRO), spin canting, metamagnetism, anisotropy, relaxation dynamics, and so on [6]. As far as LRO is concerned, some complex and exotic behaviors have been revealed in molecular systems, for example, the combination of magnetic properties and other functions [7]. The key factors in the design and synthesis of these CPs with desirable properties and expected structures are mainly focused on the appropriate selection of nodes (metal ions or metal-including clusters) and spacers (organic ligands) [8]. When organic ligands coupled with a parmagnetic metal ion, these ligands may cite peculiar magnetic behaviors e.g. (anti)ferromagnetism, magnetoelectricity and multiferroicity [9]. Among organic ligands, multidentate ligands containing carboxylate and a pyridyl group, such as nicotinate, isonicotinate, and pyridine-dicarboxylate, have been frequently used in the preparation of magnetic materials, because the various coordination modes adopted by the carboxylate group can transmit the magnetic coupling in different degrees, and the coordination of the pyridyl and carboxylate groups in these ligands may result in extended frameworks [10–14].

Meanwhile, the design, syntheses and applications of metal-organic hybrid materials based on mixed-ligands (multicarboxylate and flexible N-donor ligands) also have so far attracted unparalleled attention in research [15–17]. The flexibility of N-donor ligands can adopt different conformations and thus lead to distinct symmetries during the self-assembly process [18]. As part of our investigations on the structural diversity, magnetism properties of metal-organic hybrid materials based on mixed-ligands, herein, pyridine-3,5-dicarboxylic acid (H_2pdc) and 1,4-bis(imidazol-l-yl)butane (bib) were selected as a bridging ligand and reacted with Ni(II) ions, giving rise to a new metal-organic hybrid materials, namely $[Ni(pdc)(bib)]\cdot 2H_2O$ (**1**). Moreover, their magnetic properties were also investigated and discussed in detail.

Reaction of H_2pdc with bib and Ni(II) acetate at 140 °C for 3 days under hydrothermal conditions generates green crystalline product **1** [19]. The compositions were confirmed by elemental analysis and IR spectra, and powder X-ray diffraction. Single crystal X-ray diffraction study [20] reveals that complex **1** crystallizes in a monoclinic system with space group $P2_1/n$ and has a 3-D supramolecular framework work based on 2-D layers. All Ni sites are six-coordinated with a distorted octahedron geometry by three carboxylate-oxygen atoms (O1, O2 and O3#1, symmetry code: #1, $-x+1, y, z$) from two pdc^{2-}, one nitrogen atom (N1#2, symmetry code: #2, $-x+1/2, y+1/2,$

---

[*] Corresponding authors at: College of Materials and Chemical Engineering, China Three Gorges University, Yichang 443002, PR China.

E-mail addresses: lidongsheng1@126.com (D.-S. Li), mazhuxp@126.com (L.-F. Ma).

http://dx.doi.org/10.1016/j.inoche.2016.04.023
1387-7003/

$-z + 1/2$.) from pdc^{2-}, and two *trans*-nitrogen atoms (N2 and N5#2) from two bib ligands with the angle of N2-Ni1-N5#2 of 175.7° (Fig. S1, Supporting Information). The pdc^{2-} ligand adopts a $(\kappa^1\text{-}\kappa^1)\text{-}(\kappa^1)\text{-}(\kappa^1)\text{-}\mu_3$-bridge linking three Ni(II) ions to form a 2D layer, moreover, the bib ligand with *TGG* conformation (T = trans, G = gauche) bridge Ni(II) ions to generate a 2_1 helical chain along [010] axis with the pitch of 12.5 Å, which decorate the 2D layer at two sides in an outward fashion, resulting in a interesting helical-armed 2D network. Analysis of the network topology of **1** reveals that each Ni(II) center acts as a 5-connected node to connect three pdc^{2-} ligands and two bib spacers. And the pdc^{2-} ligands serve as the 3-connected nodes. Thus, a (3,5)-connected network with the point symbol of $(3\cdot5^2)(3^2\cdot5^3\cdot6^4\cdot7)$ is constituted (Fig. S2, Supporting Information[†]). There are evident intermolecular π···π stacking interactions between the adjacent imidazol ring of the adjacent 2D layers with co-facial distances of 3.66 and 3.78 Å (Fig. 1), which extend these 2D with ABAB stacking fashions to build final 3-D supramolecular framework (Fig. 1).

Phase purities of the bulky materials of **1** were confirmed by powder X-ray diffraction (PXRD) patterns (see Fig. S3, SI[†]). The experimental and simulated PXRD patterns agree well with each other, confirming the good phase purity. Additionally, the thermogravimetric analysis of **1** was carried out under an air atmosphere (Fig. S4, Supporting Information[†]). The first weight lost of 7.8% was observed from 115 °C to 198 °C corresponding to the lost of free water molecules (calcd. 8.0%). Then pyrolysis of the sample occurred from 325 to 490 °C. The final residue of 24.2% is close to the calculated 24.6% based on NiO.

The temperature-dependent magnetic susceptibilities were measured on polycrystalline samples of **1** at 1000 Oe in the range of 1.8–300 K in Fig. 2. For **1**, the value of $\chi_M T$ at 300 K is 1.54 cm mol^{-1} K, which is larger than the spin-only value (1.0 cm mol^{-1} K) expected for a magnetically isolated Ni(II) ion. The $\chi_M T$ value increases gradually upon cooling to ca. 35 K. Below this temperature, $\chi_M T$ value increases abruptly to a maximum of 4.69 cm^3 mol$^{-1}\cdot$K at 12.7 K. Above 15 K, the temperature dependence of $1/\chi_M$ obeys the Curie-Weiss law with $C = 1.49$ cm K mol^{-1} and $\theta = 4.91$ K, revealing dominant ferromagnetic interactions between the adjacent Ni(II) ions. Upon further cooling to 2 K, $\chi_M T$ decreases quickly. The steep declines in $\chi_M T$ at low temperature clearly indicate that a kind of spontaneous magnetization emerges. This phenomenon in a ferromagnetic system could be attributed to weak antiferromagnetism, owing to spin canting: the antiferromagnetic coupled spins from different sublattices are not parallel, but canted to each other, and the resulting net moments are correlated in a antiferromagnetic-like fashion and develop into LRO below the critical temperature.

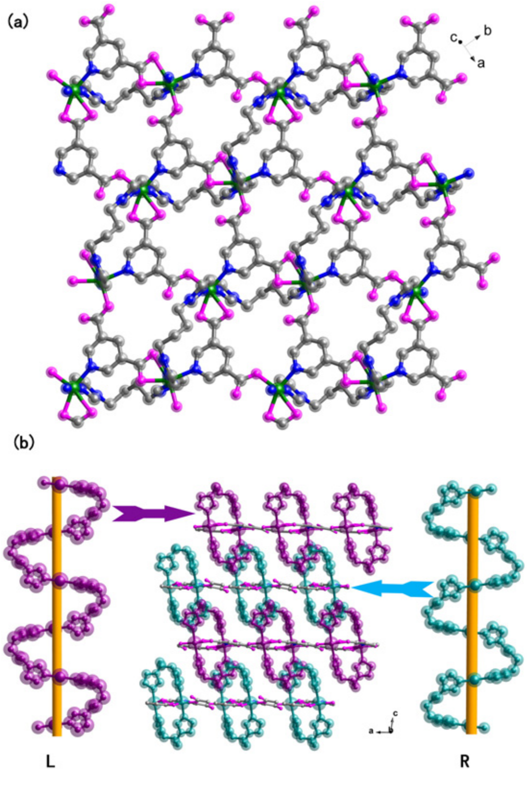

Fig. 1. (a) 2D layer in **1**. (b) 3D supramolecular structure of **1** and R- and L-handed helical chains.

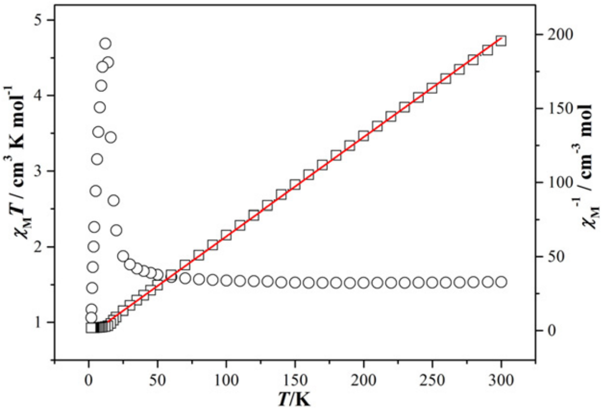

Fig. 2. Temperature dependence of $\chi_M T$ and χ_M^{-1} for **1**. Open points are the experimental data, and the solid line represents the best fit obtained from the Curie-Weiss law.

To characterize the low-temperature behaviors of **1**, FC (field-cooled) and ZFC (zero-field-cooled) magnetization measurements were performed under 50 Oe (Fig. 3a). The ZFC magnetization shows

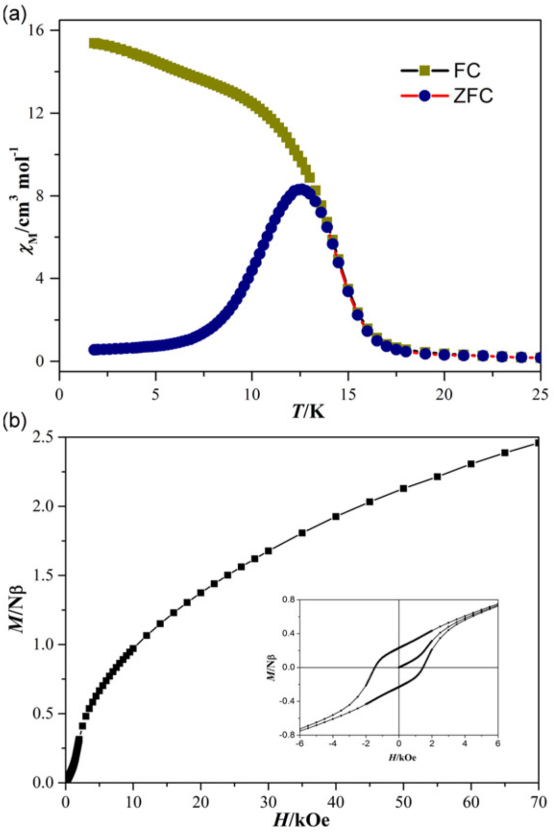

Fig. 3. (a) Low temperature dependence of the magnetic susceptibility (χ) for **1** measured under zero field cooling (ZFC) and field cooling (FC) conditions. (b) Field-dependent magnetization for **1** measured at 2.0 K. Insert: *M* versus *H* hysteresis loops for **1**.